Journal of Thermal Analysis, Vol. 41 (1994) 387-404

In celebration of the 60^{th} birthday of Dr. Andrew K. Galwey

THE NON-ISOTHERMAL DECOMPOSITION OF COBALT ACETATE TETRAHYDRATE

A kinetic and thermodynamic study

M. A. Mohamed, S. A. Halawy and M. M. Ebrahim

Department of Chemistry, Faculty of Science, Qena, Egypt

Abstract

The non-isothermal decomposition of cobalt acetate tetrahydrate was studied up to 500°C by means of TG, DTG, DTA and DSC techniques in different atmospheres of N_2, H_2 and in air. The complete course of the decomposition is described on the basis of six thermal events. Two intermediate compounds (i.e. acetyl cobalt acetate and cobalt acetate hydroxide) were found to participate in the decomposition reaction.

IR spectroscopy, mass spectrometry and X-ray diffraction analysis were used to identify the solid products of calcination at different temperatures and in different atmospheres. CoO was identified as the final solid product in N_2, and Co_3O_4 was produced in air. A hydrogen atmosphere, on the other hand, produces cobalt metal. Scanning electron microscopy was used to investigate the solid decomposition products at different stages of the reaction. Identification of the volatile gaseous products (in nitrogen and in oxygen) was performed using gas chromatography. The main products were: acetone, acetic acid, CO_2 and acetaldehyde. The proportions of these products varied with the decomposition temperature and the prevailing atmosphere.

Kinetic parameters (e.g. E and $\ln A$) together with thermodynamic functions (e.g. ΔH, C_p and ΔS) were calculated for the different decomposition steps.

Keywords: cobalt acetate tetrahydrate, IR, kinetics, MS, non-isothermal decomposition, thermodynamic study, TG-DTG-DTA-DSC, X-ray

Introduction

Thermal decomposition of metal carboxylates has for long been the subject of numerous investigations [1]. Metal acetates, especially those of the transition metals, are no exception in this respect. The importance of metal acetates arises from their occasional use for the preparation of metals and metal oxide catalysts [2]. These compounds are also common intermediates in the decomposition of metal malonates [3, 4].

John Wiley & Sons, Limited, Chichester
Akadémiai Kiadó, Budapest

A number of studies has been concerned with the decomposition of nickel acetate in different atmospheres [5, 6]. It was reported that the decomposition involves the formation of a basic nickel acetate salt, i.e. $(1-x)NiAc_2{\cdot}xNi(OH)_2$ [5]. Galwey *et al.* [7] have suggested the participation of nickel carbide, i.e. Ni_3C, as an intermediate. The prevailing atmosphere was shown to influence the type of solid product, where NiO was the final product in an oxygen atmosphere [5, 6] and Ni metal or a mixture of Ni+NiO were reported as the final products in vacuum or in N_2 [7].

Lead acetate was also found [8] to decompose through the participation of two basic salts, i.e. $PbAc_2{\cdot}PbO$ and $PbAc_2{\cdot}2PbO$. In a recent study [9] on lead acetate, we have found additionally that two melting steps occur in the decomposition process. Cadmium acetate decomposes in air to the carbonate intermediate, which later decomposes to the oxide CdO [10]. No intermediates were reported to accompany the decomposition of manganese acetate [11]. Mn_3O_4 and MnO were reported as the solid products in oxygen and in vacuum, respectively.

The main volatile gaseous products of the decomposition of these acetates were reported as CH_3COOH, $(CH_3)_2CO$ and CO_2, together with some other minor products, e.g. CO, CH_4, ketene, acetylacetone and isobutene [7, 8, 10].

Cobalt acetate, which is known as an auto-oxidation catalyst and as a bleaching and drying agent for varnishes and lacquers [12], has received relatively little attention. In an isothermal study, under vacuum, the α-time curves were irreproducible [6], which was ascribed to sublimation. Baraldi [11] has identified Co_3O_4 as the final product of decomposition in air, while a mixture of Co+CoO was formed in vacuum. No intermediate compounds were reported for the decomposition of cobalt acetate [11].

The present work is intended to examine the complete decomposition course of cobalt acetate tetrahydrate up to 500°C in different dynamic atmospheres. The effect of the prevailing atmosphere on the product distribution was also studied. It also extends our previous studies [9] on the decomposition of metal acetates.

Experimental

Material

Cobalt acetate tetrahydrate, $Co(CH_3COO)_2{\cdot}4H_2O$, used in the present study, was an analytical grade material (Fluka AG, Switzerland). It was used without any further treatment, except for a gentle crushing to get a uniform particle size.

Instruments

Thermogravimetry (TG), differential thermal analysis (DTA) and differential scanning calorimetry (DSC) measurements were performed, using Shimadzu Thermal Analyser Instruments (TGA-50H, DTA-50 and DSC-50), Japan. These were equipped with a data acquisition and handling system (Shimadzu C-R4AD).

Measurements were carried out in different dynamic atmospheres of dry N_2, air and H_2 (flow rate = 40 ml/min). Highly sintered α-Al_2O_3 powder (Shimadzu Co.) was the reference material used for the DTA and DSC measurements. The heat of transition of specpure indium metal (28.24 Jg^{-1} [14]), Johnson Matthey, at 157°C was used for the DSC calibration.

Infrared (IR) absorption spectra of the parent salt and its decomposition products in N_2 (or in air) were taken from KBr-supported test samples using a model 1430 Perkin-Elmer ratio-Recording IR spectrophotometer.

X-ray powder diffraction analysis of cobalt acetate and its solid products of decomposition in N_2 (and in air) was carried out by means of a mode JSX-6OPA JEOL X-ray diffractometer (Japan) using Ni-filtered CuK_α radiation.

Mass spectrometric analysis was used to identify the composition of some intermediates that may be formed during the decomposition process. This was carried out by means of a model GCMS sp. 1000 Shimadzu (Japan).

Volatile decomposition products of the partially dehydrated salt were separated, in a stream (85 ml/min) of dry N_2 or oxygen, using a 2 m long column packed with 10% PEG/Shimalite TPA, at 150°C. They were, then, qualitatively and quantitatively determined by means of a model 14-A Shimadzu computerized gas chromatograph, equipped with an automatic gas-sampling valve (type HGS-2), a thermal conductivity detector (TCD) and a data acquisition and handling system (Shimadzu C-R4AD).

Scanning electron microscopy (SEM) was used to investigate the residual solid products of cobalt acetate decomposition at some selected temperatures, using a model JSM T-2000 JEOL scanning electron microscope (Japan).

Data processing

Kinetic parameters, the activation energy (E, $kJ\cdot mol^{-1}$ and the frequency factor $\ln A$), were calculated for the decomposition processes observed, using the Kissinger equation [14]:

$$\ln \varphi/T^2 = -E/RT + \ln AR/E$$

where φ is the heating rate ($deg\cdot min^{-1}$).

Calculations of the kinetic and thermodynamic parameters are discussed in detail elsewhere [15].

Results and discussion

Thermal analysis

Thermogravimetry (TG)

Four different heating rates were used (5, 10, 15 and 20 deg·min^{-1}). Figure 1 shows TG, DTG and DTA curves of the decomposition of cobalt acetate tetrahydrate in N_2 at 5 deg·min^{-1}.

The TG curve displays four mass loss steps between 30–375°C. The first of these takes place between 30–140°C and is accompanied by a mass loss of 20.3%. This is almost equivalent to the loss of 3 molecules of water (expected mass loss = 21.7%). There is a gradual mass loss of about 1–2% at 220°C, followed by the second marked mass loss step (3.5%), with DTG maximum at 245°C. This is followed by the third step which commences at 264°C and is associated with a 7.6% mass loss. The fourth, and last, step commences at 313°C and is accompanied by a 30.95% mass loss, which brings the total mass loss up to 64.7% of the original sample mass (this value varied, for a number of experiments, between 64–67%).

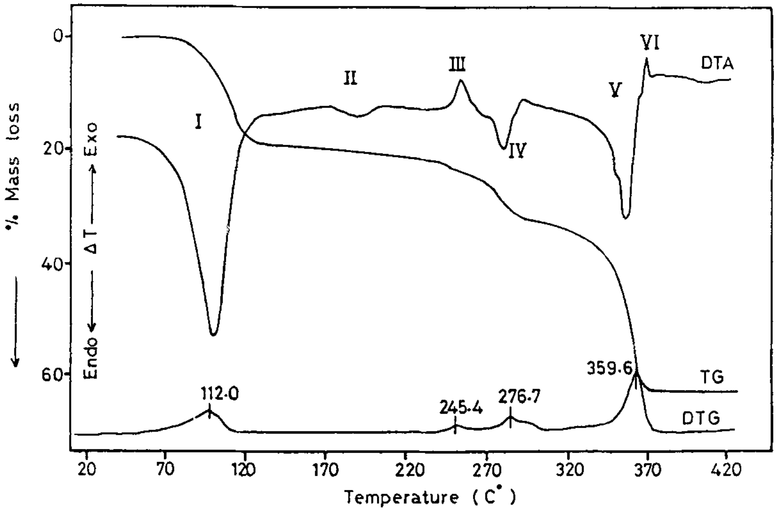

Fig. 1 TG, DTG and DTA curves for the decomposition of cobalt acetate tetrahydrate performed at 5 deg·min^{-1} in a dynamic atmosphere of N_2

The total mass loss in air was found to be 66.7%, which suggests that Co_3O_4 is the eventual decomposition solid product. In H_2 atmosphere, however, the observed total mass loss (ca. 72.51%) suggests that cobalt metal is produced (expected value is 76%).

Temperatures at which the mass loss steps are maximized (T_{max}) were determined from DTG curves. Figure 1 shows four maxima for the DTG curves located at 112, 254.4, 276.7 and 359.6°C. The results obtained as a function of heating rate, in N_2, are summarized in Table 1. Generally, T_{max} values were shifted towards higher values as the rate of heating (φ) increases.

Differential thermal analysis (DTA)

Differential thermal analysis (DTA) was also carried out in three different atmospheres (N_2, H_2 and air) and at five different heating rates (ca. 5, 7, 10, 15 and 20 $deg \cdot min^{-1}$).

Figure 1 shows that the DTA curve monitors six thermal events (labelled I–VI) maximized at 114.1 (endo), 190.8 (endo), 247.6 (exo), 272.3 (endo), 350.3 (endo) and 363.5°C (exo), respectively. Endotherm-I is attributed to the dehydration of the tetrahydrated salt to approximately the monohydrate. The broad, weak, endotherm-II is associated with the gradual mass loss which followed the dehydration process. Exotherm-III corresponds to the second mass loss step (3.5%) and, similarly, endotherm-IV is attributed to the third mass loss step (7.6%). Endotherm-V is related to the last, fourth, mass loss step which involves about 31% of the original sample mass. The last sharp exotherm-VI is accompanied by no mass loss which suggests a physical process (possibly recrystallization of the oxide product).

The effect of variation of heating rate (φ) on the maximum temperature (T_{max}) of the DTA peaks is shown in Table 2. Some of these peaks (e.g. peaks II and III) vanished at higher rates of heating. Data from Table 2 were used to calculate the activation energy (E, $kJ \cdot mol^{-1}$) and the frequency factor ($\ln A$) for each process form the linear plots of $\ln \varphi/T^2$ against $1/T$, as described above. The correlation coefficient for each line was also calculated. Values of the kinetic parameters thus obtained are listed in Table 3. The effect of different atmospheres on the decomposition of cobalt acetate is shown in Fig. 2 where three DTA curves are displayed. These were performed in N_2, H_2 and in air (all at 5 $deg \cdot min^{-1}$).

The DTA curve performed in H_2 is broadly similar to that carried out in N_2, except for the following modifications: (i) the endothermic peak-V has been shifted toward a lower temperature (from 350°C in N_2 to 291°C in H_2) due to the reduction to form metallic cobalt and (ii) the last exotherm-VI (in N_2) disappears completely in H_2 atmosphere.

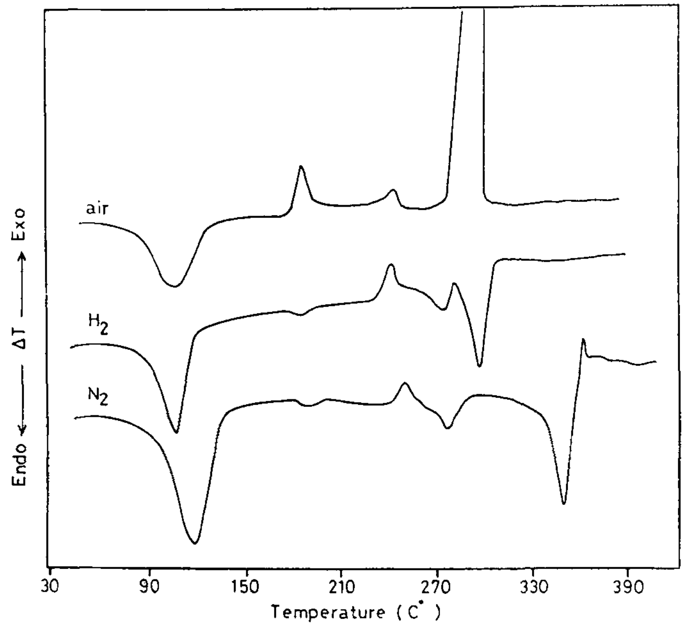

Fig. 2 Three DTA curves performed at 5 deg·min^{-1} in different atmospheres of nitrogen, hydrogen and in air

In air, however, peak-II shows an exothermic nature (instead of the endothermic nature shown in N_2 and in H_2), which appears to compensate for the original endotherm (i.e. the exothermic reaction is stronger than the original endothermic step). This could be due to oxidation of the decomposition products observed to form in nitrogen or to the formation of a stable coordination compound with oxygen. In addition, the last three peaks (IV–VI) have appeared, here, as one very strong exotherm which is ascribed to the oxidation to form Co_3O_4. Generally, the decomposition in hydrogen and in air has been completed at a markedly lower temperature (ca. 60–70°C) than in an atmosphere of N_2.

Differential scanning calorimetry (DSC)

Differential scanning calorimetry (DSC) measurements were used to calculate thermodynamic functions such as the enthalpy (ΔH, kJ·mol^{-1}), heat capacity (C_P, kJ·K^{-1}·mol^{-1}) and the entropy change (ΔS, J·K^{-1}·mol^{-1} for each thermal event in the decomposition course (under N_2 atmosphere). These values are given in Table 3.

Table 1 Summary of the TG and DTG results for the decomposition of cobalt acetate tetrahydrate in nitrogen atmosphere

Heating rate (Φ) / deg·min^{-1}	1st step Temperature range / °C	*ML%	**T_{max} / °C	2nd step Temp. range / °C	ML%	T_{max} / °C	3rd step Temp. range / °C	ML%	T_{max} / °C	4th step Temp. range / °C	ML%	T_{max} / °C
5	30–140	20.30	112	238–264	3.42	245	264–295	7.56	277	313–372	30.95	360
10	53–150	20.60	123	241–275	4.40	261	274–299	7.20	284	318–394	32.43	369
15	49–152	20.16	133	260–278	3.10	270	278–308	8.45	291	334–400	30.37	375
20	60–160	20.19	140	270–311	4.10	282	282–315	8.07	303	339–410	30.70	385

*ML = Mass loss

**T_{max} = Peak maximum temperatures from DTG curves

Table 2 Summary of the DTA results

Heating	T_{max} / °C					
rate /	endo	endo	exo	endo	endo	exo
deg·min^{-1}	I	II	III	IV	V	VI
5	114.1	190.8	247.6	272.3	350.3	363.5
7	114.9	191.2	250.0	273.1	352.3	368.3
10	120.9	191.7	253.2	274.4	359.4	379.1
15	125.4	196.3	–	278.5	364.6	387.8
20	131.2	–	–	284.7	372.0	396.8

Table 3 Summary of the kinetic and thermodynamic parameters (in N_2)

Parameter	endo I	endo II	exo III	endo IV	endo V	exo VI
E/kJ·mol^{-1}	92.41	291.05	263.60	272.99	195.60	133.11
ln (A/min^{-1})	27.92	75.67	60.66	59.80	36.67	24.48
Cor. coeff.	0.978	0.861	0.997	0.950	0.985	0.995
ΔH/kJ·mol^{-1}	129.50	2.24	– 9.96	19.93	54.80	– 2.99
C_p/kJ·mol^{-1}·K^{-1}	1.43	0.08	0.36	0.50	1.20	2.99
ΔS/J·mol^{-1}·K^{-1}	350.00	5.00	–20.00	37.00	88.00	–94.00

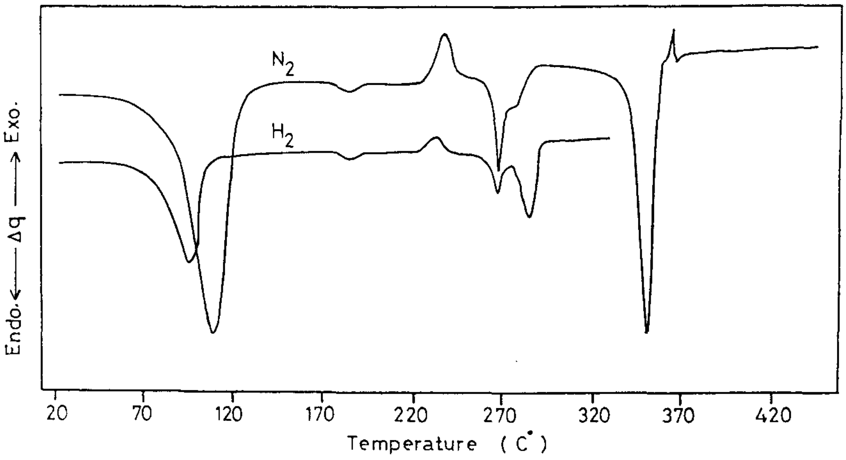

Fig. 3 Two DSC curves performed at 5 deg·min^{-1}, one in nitrogen atmosphere and the other in hydrogen

Figure 3 shows two DSC curves, one was performed in N_2, the other in H_2. The similarity between the DSC and DTA curves is obvious. The effect of the hydrogen atmosphere on the decomposition of cobalt acetate is, also, reflected in DSC curve (Fig. 3).

Product analysis

Solid phase products

(a) Infrared spectroscopy (IR): Figure 4 shows the IR spectra taken, between 4000–650 cm^{-1}, for the original cobalt acetate tetrahydrate (a) and its decomposition solid products at 210 (b), 235 (c), 260 (d) and 345°C (e) for 2 h in N_2.

Spectrum (a) of the unreacted salt shows a strong absorption peak at 3350 cm^{-1}, which is ascribed to water of crystallization [16]. Another sharp peak at 680 cm^{-1} is attributed to the acetate anion [17]. The absorption peaks at 1450 and 1030 cm^{-1} are ascribed to δ-CH_3 and pr CH_3 respectively [18].

Spectrum b (product at 210°C) is rather similar to that of the original salt (spectrum a), except that the absorption peaks get broader and the splittings get weaker. A broad band between 3000–3700 cm^{-1} is attributed to the remaining molecule of water of crystallization. In addition, a weak absorption at 2950 cm^{-1} is ascribed to ν-CH_3 [17].

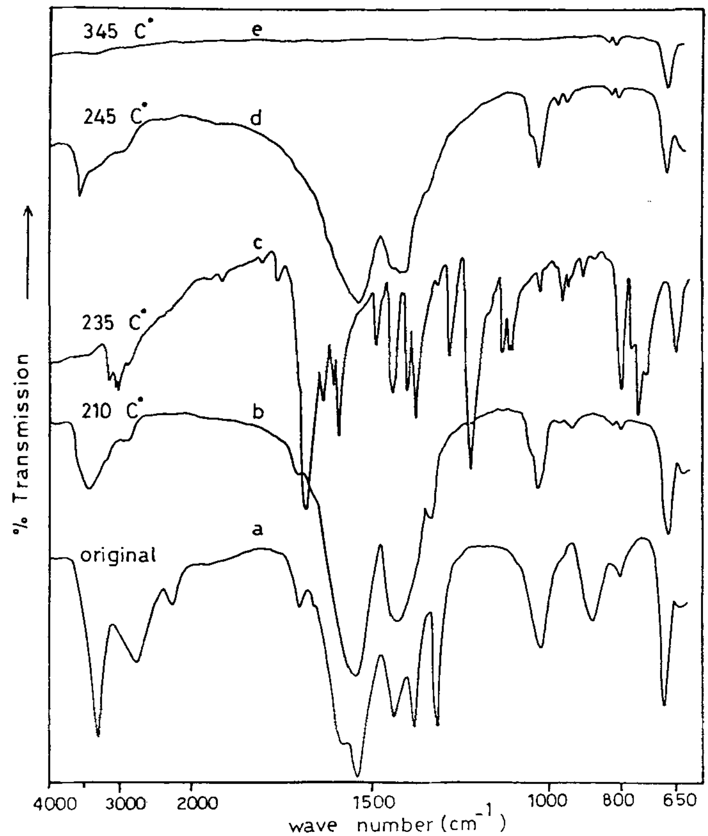

Fig. 4 IR transmission spectra of cobalt acetate tetrahydrate and its decomposition solid products (in N_2) at different temperatures

On heating the sample to 235°C (spectrum c), a group of sharp peaks has appeared, e.g. at 1290 cm^{-1} (C–CH_3), 1110, 1120 cm^{-1}. These peaks are ascribed to the asymmetric stretching vibration of aliphatic ester [19]. A very important feature is shown here where two different types of C=O stretching absorptions appeared. The first, very strong and sharp, is located at 1685 cm^{-1} which is ascribed to an acetyl CH_3C=O. The second peak at 1756 cm^{-1} is rather weak and is attributed to an ester C=O type [19].

Spectrum d (product at 245°C) is, again, similar to that recorded at 210°C, spectrum b, except that a sharp peak appeared at 3552 cm^{-1} instead of the broad band of the OH stretching of water of crystallization. This is attributed to the formation of OH groups which are known [18] to give rise to sharp bands at 3700–3500 cm^{-1}. There is also a weak absorption at 2950 cm^{-1} due to CH_3 stretching.

On heating the sample to 345°C (spectrum e), all absorption peaks have almost disappeared, except for the sharp peak at 660 cm^{-1}, which can be ascribed to stretching vibrations of the metal-oxygen bond [20].

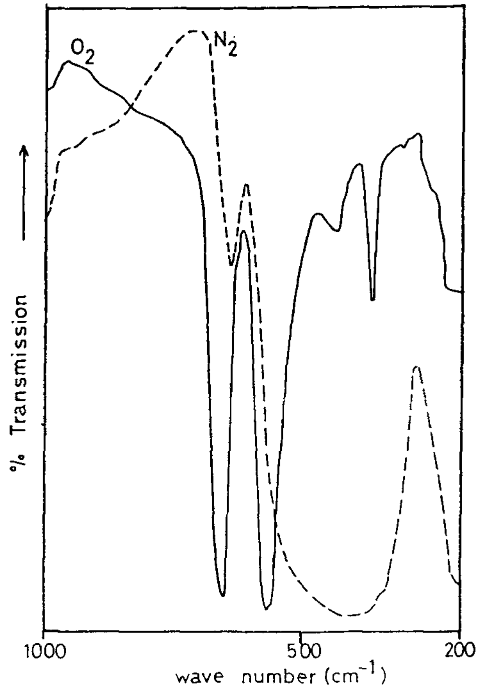

Fig. 5 IR spectra of the solid products formed on heating cobalt acetate at 400°C in nitrogen and in hydrogen

Figure 5 shows IR spectra, that were taken for the solid products on heating the acetate at 400°C in air and in nitrogen. It is clear that the prevailing atmosphere does influence the type of oxide produced. The spectrum of the sample produced in air exhibits characteristic absorptions at 665, 635, 562, 460 and 350 cm^{-1} due to Co_3O_4 [20]. In N_2, CoO is produced with its characteristic absorptions at 650 and between 560–340 cm^{-1} [21].

X-ray diffractometry

Figure 6 shows XRD patterns for the solid decomposition products of cobalt acetate at 235 (a), 340 (b), 400°C (c) in N_2, as well as ASTM data for cobalt (II) oxide CoO (d) and Co_3O_4 (e).

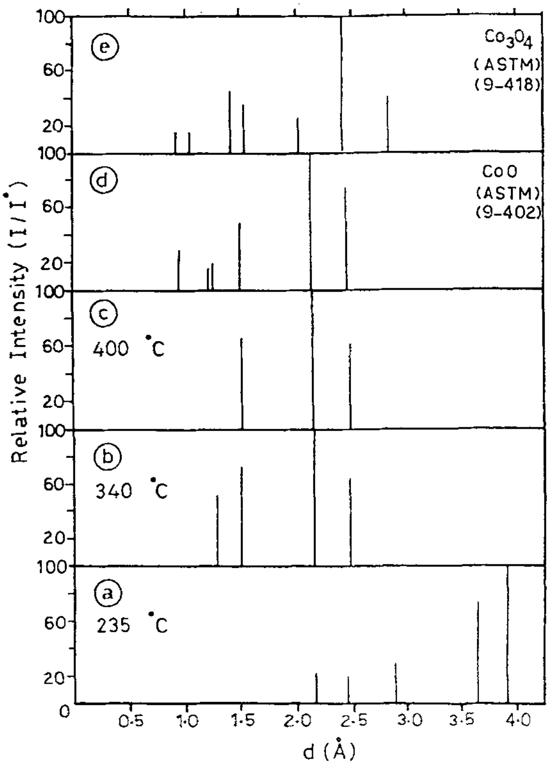

Fig. 6 X-ray diffraction patterns for the solid decomposition products of cobalt acetate at different temperatures together with the ASTM data for CoO and Co_3O_4

Pattern (b) shows that CoO began to form showing its characteristic d-spacings (ASTM card no. 9–402). The oxide crystallinity improves with increasing decomposition temperature (see pattern c).

The 235°C products shows a different pattern (a) from that of the original cobalt acetate tetrahydrate (ASTM card no. 14–718) and those of the products at 340 (pattern b) and 400°C (pattern c). This indicates the formation of an intermediate compound at 235°C which supports the IR results discussed above.

In the atmosphere of air, however, X-ray analysis showed a progressive formation of Co_3O_4 with increasing the calcination temperature. This also agrees with the IR results, since the latter could account for the formation of CoO and Co_3O_4 in N_2 and air, respectively.

Mass spectrometry

The intermediate compound formed at 235°C was subjected to mass spectrometric analysis. A pronounced peak at *m/e* = 43 (85%), corresponding to the CH_3CO group, was detected. This supports the IR and XRD results which suggested the formation on acetyl cobalt acetate.

Gas phase products

The main volatile decomposition products of cobalt acetate, after dehydration, were identified, using GC, to be acetone, acetaldehyde, acetic acid and CO_2 in either atmospheres (i.e. nitrogen or oxygen).

Scanning electron microscopy (SEM)

SEM was used to investigate cobalt acetate salt and its decomposition solid products in N_2 atmosphere. Figure 7 shows five representative micrographs (a–e) of different stages throughout the decomposition.

Micrograph (a) shows some crystallites of the original unreacted salt. These are characterized by an elongated shape with a square cross-section. The surface of these crystallites is shown to be rough with some broken areas.

Micrograph (b) represents a sample that was heated at 150°C (i.e. after dehydration). It is obvious that the dehydration has resulted in parallel cracks and laminar structures.

On heating to 300°C (micrographs c and d), crystals have suffered extensive damage. Two features are seen here. There are rounded structures in different parts of micrograph c and the presence of small pores with, again, rounded edges (micrograph d). This may indicate the possible participation of local melting [22] during the course of decomposition. The second feature is the appearance of small needle-shaped crystallites (micrograph d).

Micrograph (e) shows the solid product formed on heating cobalt acetate at 400°C in N_2. These crystallites represent CoO thus produced.

Conclusions

The course of decomposition of cobalt acetate tetrahydrate in nitrogen atmosphere can be described on basis of the experimental results discussed above. The six thermal events which were seen in the DTA and DSC curves are explained as follows:

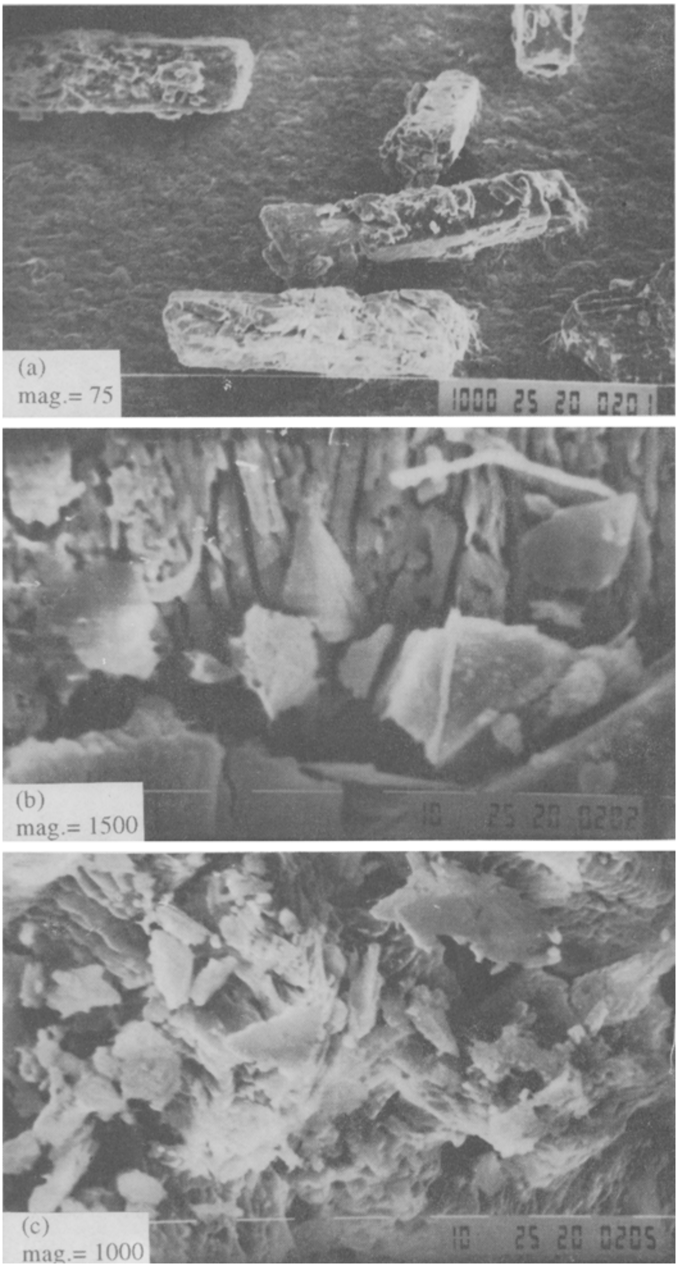

Fig. 7a Scanning electron micrographs of samples of the parent cobalt acetate tetrahydrate (a), dehydrated sample (b), solid product of decomposition on heating at 300°C (c) final solid residue at 400°C

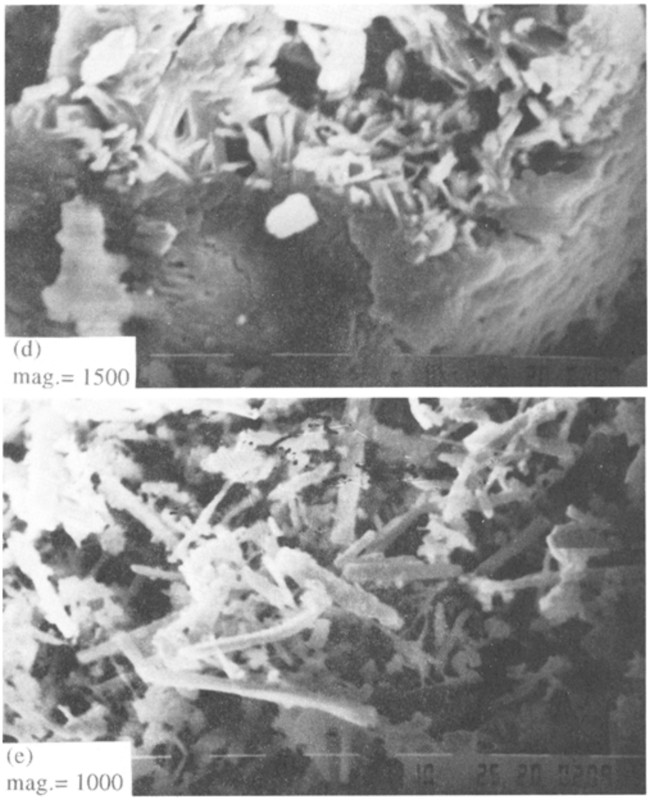

Fig. 7b Scanning electron micrographs of samples of the parent cobalt acetate tetrahydrate (d) the final solid residue at 400°C (e), heating was carried out in nitrogen

Event-I (30–140°C)

An endothermic process, accompanied by 20–21% mass loss, which is attributed to the dehydration of the tetrahydrate. The mass loss determined suggests the elimination of three moles of water to give monohydrated cobalt acetate. The activation energy (E) calculated for the dehydration, 92.4 kJ·mol^{-1}, is comparable to that reported for nickel acetate, 93 kJ·mol^{-1} [23].

Event-II (168–195°C)

A weak, rather broad, endotherm which is associated with the highest E value (291 kJ·mol^{-1}) and is accompanied by a small mass loss (ca. 1–2%). This process is attributed to a possible bulk restructuring of the monohydrate, together, with slight decomposition acetic acid was detectable in the surrounding atmosphere.

In an atmosphere of air, this event was hidden by the strong exotherm (Fig. 2). This means that the exothermic reaction was stronger than the original endothermic process.

Event-III (223–251°C)

A process that is exothermic in all atmospheres (i.e. N_2, air or H_2) and is accompanied by a 3–4% mass loss. Mass spectrometry and IR spectroscopy, Fig. 4 spectrum c, showed the formation of a new compound containing two different types of carbonyl groups. This event is, therefore, assigned to the formation of an acetyl cobalt acetate intermediate, i.e. $(CH_3COO)_2Co{\cdot}COCH_3$. X-ray diffraction (Fig. 6) showed also a new pattern, although this could not be identified, for the sample that was heated at 235°C. This, again, suggests the formation of an intermediate compound. Hydrogen enhanced this process since T_{max} in H_2 shifted towards a lower value (232°C) than in N_2 (247.5°C). This could be explained as being a hydrogen-facilitated formation of acetyl groups from acetic anhydride, via the liberation of acetic acid.

Event-IV (250–290°C)

This was an endothermic process, whether in N_2 or H_2 atmospheres. IR results, Fig. 4 spectrum d, indicated the presence of hydroxyl groups. Thus, this step may be attributed to the formation of cobalt acetate hydroxide as follows:

$$Co(CH_3COO)_2{\cdot}COCH_3[+H_2O] \rightarrow (CH_3COO)_2Co{\cdot}OH + CH_3CHO$$

Consistent with this, the gas chromatography experiments identified acetaldehyde in the volatile products.

It should be noted here that E values measured for events 3 and 4 are relatively high (263 and 273 kJ·mol^{-1}, respectively), see Table 3.

Event-V (between 315–360°C)

This event is accompanied by the largest mass loss (≈31%) observed. It represents the autocatalytic decomposition of the adsorbed acetate and other related species on the surface of cobalt oxide. The reaction in N_2 was accompanied by a remarkable increase in the proportion of acetic acid in the gas phase. This is evidence of a proton transfer step and explains the observed enhancing effect of hydrogen atmosphere for that event. T_{max} has been shifted some 70°C lower than its value in N_2 (350°C in nitrogen and 284°C in hydrogen).

The autocatalytic properties of the cobalt oxide product in the temperature range of event-V were examined by GC. Acetone was passed over the residual solid of the event and acetic acid was the product.

The activation energy value for that process (195 $kJ \cdot mol^{-1}$) was again comparable with those measured for lead and nickel acetates, 172 and 170 $kJ \cdot cm^{-1}$ respectively [9, 23].

Event-VI (370–390°C)

A sharp exotherm which is accompanied by no mass loss. It suggests a recrystallization of CoO thus produced. This process appeared in N_2 atmosphere only. In an atmosphere of hydrogen, however, this process completely disappeared, since cobalt metal is the final solid product.

References

1 M. E. Brown, D. Dollimore and A. K. Galwey, Reactions in the Solid State (Comprehensive Chemical Kinetics, vol. 22), C. H. Bamford and C. F. H. Tipper (Eds), Elsevier, Amsterdam 1980.
2 D. L. Trimm, Design of Industrial Catalysts, Chemical Engineering Monograph II, Elsevier, Amsterdam 1980.
3 A. K. Galwey, S. G. McKee, T. R. B. Mitchell, M. A. Mohamed, M. E. Brown and A. F. Bean, Reactivity of Solids, 6 (1988) 203.
4 A. K. Galwey and M. A. Mohamed, Solid State Ionics, 42 (1990) 135.
5 A. M. Gadalla and H. Fu Yu, Thermochim. Acta, 164 (1990) 21.
6 J. Leicester and M. J. Redman, J. Appl. Chem., 12 (1962) 357.
7 A. G. Galwey, S. G. McKee, T. R. B. Mitchell, M. E. Brown and A. F. Bean, Reactivity of Solids, 6 (1988) 173.
8 R. Leibold and F. Huber, J. Thermal Anal., 18 (1980) 493.
9 M. A. Mohamed, S. A. Halawy and M. M. Ibrahim, Submitted for publication.
10 S. A. A. Mansour, G. A. M. Hussein and M. I. Zaki, Reactivity of Solids, 8 (1990) 197.
11 P. Baraldi, Spectrochim. Acta, 38A (1982) 51.
12 Comprehensive Inorg. Chem. vol. 3, J. C. Bailar, H. J. Emeleus, R. Nyholm and A. F. Trotman-Dickenson (Eds), Pergamon Press, Oxford 1975.
13 R. C. Weast (Ed.), Handbook of Chemistry and Physics (62nd edn), CRC Press, Florida, 1982.
14 H. E. Kissenger, Anal. Chem., 29 (1957) 1702.
15 M. A. Mohamed and S. A. Halawy, J. Thermal Anal., 41 (1994) 147.
16 S. F. Dyke, A. J. Floyed, M. Sainsbury and R. S. Theobald, Organic Spectroscopy- An Introduction (2nd edn), Longman, London 1978.
17 J. R. Ferraro, Low Frequency Vibration of Inorganic and Coordination Compounds, Plenum Press, New York 1971.

18 K. Nakamoto, Infrared Spectra of Inorganic and Coordination Compounds, J. Wiley and Sons, London 1963.
19 R. L. Pecsok, L. Shields, T. Cairns and T. G. McWilliam, Modern Methods of Chemical Analysis, 2nd edn, J. Wiley and Sons, London 1976.
20 N. T. McDevitt and W. L. Baun, Spectrochim. Acta, 20 (1964) 799.
21 R. A. Nyquist and R. O. Kogal, Infrared Spectra of Inorganic Compounds, Academic Press, New York 1971, p. 219.
22 A. K. Galwey, M. A. Mohamed and D. S. Cromie, Reactivity of Solids, 1 (1986) 235.
23 M. A. Mohamed, S. A. Halawy and M. M. Ebrahim, J. Anal. and Appl. Pyrolysis, in press.

Zusammenfassung — In verschiedenen Atmosphären aus N_2, H_2 und in Luft wurde mittels TG, DTG, DTA und DSC bis zu 500°C die nichtisotherme Zersetzung von Kobaltacetat-Tetrahydrat untersucht. Der gesamte Umsetzungsprozeß wird auf der Grundlage von sechs thermischen Ereignissen beschrieben. Man fand, daß zwei Zwischenprodukte (Acetylkobaltacetat und Kobaltacetathydroxid) an den Zersetzungsreaktionen beteiligt sind.

Die Bestimmung der Feststoffprodukte der Kalzinierung bei verschiedenen Temperaturen und in verschiedenen Atmosphären erfolgte mittels IR-Spektroskopie, Massenspektrometrie und Röntgendiffraktion. In Stickstoff entsteht als festes Endprodukt CoO, in Luft hingegen Co_3O_4. In Wasserstoffatmosphäre kommt es jedoch zur Bildung von metallischem Kobalt. Mittels Scanning-Elektronenmikroskopie wurden die festen Zersetzungsprodukte zu verschiedenen Reaktionsstadien untersucht. Die Bestimmung flüchtiger gasförmiger Produkte (in Stickstoff und in Sauerstoff) erfolgte mittels Gaschromatographie. Die Hauptprodukte waren: Aceton, Essigsäure, CO_2 und Acetaldehyd, deren relative Menge von der Zersetzungstemperatur und der vorherrschenden Temperatur abhängt.